Brillouin scattering in incommensurate Rb_2ZnBr_4 and Rb_2ZnCl_4

J. J. L. Horikx, A. F. M. Arts, J. I. Dijkhuis, and H. W. de Wijn
Fysisch Laboratorium, Rijksuniversiteit Utrecht, P.O. Box 80 000, 3508 TA Utrecht, The Netherlands
(Received 13 October 1987; revised manuscript received 21 July 1988)

In Rb_2ZnBr_4 and Rb_2ZnCl_4, Brillouin scattering of longitudinal-acoustic phonons is performed as a function of the temperature. Small anomalies, arising through a coupling with the soft-going modes, are observed in both the phonon velocity and damping near the transition from the orthorhombic to the modulated phase. The anomalies are quantitatively accounted for with a comprehensive analysis based on an adaptation of Levanyuk's Landau theory for sound absorption near second-order phase transitions. In the incommensurate regime, two mechanisms appear to contribute by about equal weights: an effective coupling bilinear in the strain and amplitude fluctuations, and a coupling linear in the strain, but quadratic in the amplitude fluctuations. Above the transition, the soft-mode counterpart of the latter coupling remains. Estimates of these contributions derived from the theory with parameter values from other sources are found to be in conformity with the experiment. The analysis further yields the amplitude-mode and soft-mode relaxation times as well as the transition temperatures. Additionally, the anomalous phonon velocity and damping observed in Rb_2ZnBr_4 near a transition at 115 K are analyzed. Finally, the elastic constants of Rb_2ZnBr_4 and Rb_2ZnCl_4 are determined at 300 K.

I. INTRODUCTION

This paper is concerned with a detailed experimental investigation of the frequency and damping of longitudinal-acoustic phonons in Rb_2ZnBr_4 and Rb_2ZnCl_4 by means of Brillouin spectroscopy, and with a comprehensive interpretation of the results in terms of a phenomenological Landau theory. Both systems, as well as a few other compounds having the β-K_2SO_4 structure, are of interest because they undergo a transition from a high-temperature normal phase to a displacively modulated phase. In its normal phase, Rb_2ZnBr_4 is orthorhombic with space group $D_{2h}^{16}=Pmcn$ (choice of axes such that $b>c>a$) and paraelectric.[1-3] Below $T_1=353$ K, the structure becomes modulated with a nearly temperature-independent wave vector $\mathbf{q}_0=(\frac{1}{3}-\delta)\mathbf{c}^*$, with $\delta\approx 0.04$,[4-7] but remains paraelectric. At the lock-in transition at $T_2=194$ K, the parameter δ drops to zero. An orthorhombic commensurate structure with space group $C_{2v}^9=P2_1cn$ results, whose unit cell is tripled in length along the c axis in comparison with the normal phase.[7] This structure is ferroelectric along the a axis.[1-3,8] Additional transitions have been found at $T_3=115$ K, $T_4=76$ K, and $T_5=50$ K with specific-heat,[9] NMR,[10] x-ray,[7] and dielectric[3,11] experiments. Between T_3 and T_4, Rb_2ZnBr_4 is observed to be antiferroelectric along the b axis, while the ferroelectric order along the a axis extends from T_2 down to below 30 K.[3] In the compound Rb_2ZnCl_4, isostructural with Rb_2ZnBr_4, the transition from the normal to the incommensurate phase takes place at $T_1=304$ K.

Brillouin scattering, like ultrasonic techniques, probes the coupling between the order parameter and the strains through its effects on the elastic behavior. In the present cases, the order parameter may be identified with the averaged coordinate $Q(\mathbf{q}_0)$ of the soft-phonon mode invoking the transition to the modulated phase.[12] The associated acoustic anomalies of the frequency and linewidth are inherently small, and can only be retrieved with a careful analysis correcting for the instrumental profile and the finite range of scattering angles. This is done below to find that the anomalies are of order 1% only. The elastic properties of Rb_2ZnCl_4 have previously been investigated with ultrasonic techniques[13,14] and Brillouin scattering.[15-17] Brillouin scattering was, however, restricted to frequency shifts.

In the interpretation in terms of a phenomenological Landau theory, the objective is to achieve a quantitative account of the frequency and linewidth anomalies at both sides of the transition. To this end, terms up to second order in the order-parameter fluctuations need be retained in the expansion of the interaction between the order parameter and the strains. The formalism developed below is an adaptation of the theory by Levanyuk[18] for sound absorption near second-order phase transitions, as applied by Yao *et al.*[19] to the case of the ferroelectric-ferroelastic phase transition in terbium molybdate. In the equations of motion of the acoustic modes, terms quadratic in the order-parameter fluctuations appear to account for the elastic anomalies above the transition. Below the transition, however, the anomalies are made up, in about equal portions, of the quadratic terms and terms bilinear in the order-parameter fluctuations and the strain. The present treatment explicitly takes the quadratic terms into consideration, and in this respect goes beyond previous analyses of Brillouin anomalies in incommensurate systems, notably K_2SeO_4.[20-23]

II. EXPERIMENTAL

The Brillouin spectrometer is of conventional design. As light source an argon-ion laser operating in a single

mode at a wavelength of 514.5 nm and at a power level of 100 mW or less is used. The incident beam is focused, with suitable polarization, onto the sample to a diameter of about 80 μm. The scattered light is analyzed by means of an actively stabilized triple-pass Fabry-Perot interferometer (Burleigh RC 110 with DAS 1 digital data acquisition and stabilization unit, but with the high-voltage supplied externally for greater stability), operating at a free spectral range of about 6 GHz with a finesse of 50 to 60. All data have been taken in a $90°\pm1°$ scattering geometry. Stray light is reduced with a second collimator, following the interferometer. To eliminate low-lying Raman lines, a grating monochromator with a bandwidth of about 8 cm^{-1} is employed as a filter. The analyzed light is detected with a cooled photomultiplier ($S20$ photocathode), whose output is fed to standard photon-counting equipment providing digital input signals for the DAS 1. The background signal is approximately 1 count/s. Typical runs consist of 500 to 2000 scans over 512 channels, with a channel dwell time of 1 ms, increased to 20 ms when scanning through the Brillouin peaks. The free spectral range has been calibrated with reference to the Brillouin shifts of the [110] longitudinal- and transverse-acoustic phonons in KCl, which from the known elastic constants and refractive indices[24] are calculated to amount to 15.960 and 7.315 GHz, respectively. The calibration error is estimated to be 0.5%, mainly residing in the uncertainty of the scattering angle.

Single crystals of Rb_2ZnBr_4 and Rb_2ZnCl_4, approximately 4 cm^3 in volume, have been grown with the Stockbarger method under a nitrogen atmosphere, with the melt crystallizing at a rate of 3 mm/h. They are transparent and colorless, and possess cleavage planes perpendicular to the b axis with a spread of approximately one degree of arc. The structure has been checked with x-ray diffraction. For use in the Brillouin-scattering experiments, specimens of approximately $3\times4\times5$ mm^3 in size have been cut from these crystals as necessary for the various scattering geometries, i.e., such that the incoming and outgoing beams are both perpendicular to crystal faces. The specimens have been mounted in an optical cryostat to a precision of about one degree of arc in their orientations. The temperature of the mount is regulated to within 0.02 K. Temperatures have been measured with a calibrated platinum resistor. Sample heating due to the laser beam is estimated to be less than a few tenths of a Kelvin.

In the analysis of the Brillouin peaks, the peak position, the phonon-induced broadening, and the peak height are taken as adjustable parameters. The anomalous Brillouin frequency shifts and damping rates of acoustic phonons in Rb_2ZnBr_4 and Rb_2ZnCl_4 typically are a fraction of the instrumental width only. In carrying out the fits, therefore, we first determine, separately for each spectrum, an *effective* instrumental profile by convoluting the bare instrumental profile, as measured from the unshifted line, with the distribution of Brillouin frequency shifts associated with the finite acceptance angle. A Lorentzian with a width corresponding to the phonon lifetime is in turn convoluted with this effective instrumental profile, and the result is fitted to the observed Brillouin peaks. The fits appear to be of excellent quality, as is exemplified in Fig. 1. All double convolutions have been evaluated numerically, repeatedly in the course of the fitting. As it appeared, the bare instrumental profile is adequately parametrized with a Lorentzian to a power p varying between 2.3 and 2.9 (see fits to the Rayleigh lines in Fig. 1), compared to a p of exactly 3 for an ideal triple-pass instrument. Even in the case of optimal alignment, however, mirror imperfections, the finite acceptance angle, the active stabilization of the interferometer, and the residual instability of the laser frequency within the interferometer stabilization time (~10 s) all tend to raise the wings of the transmission profile at the expense of its central peak, thereby reducing the fitted p. Further, the uncertainty in p is substantial due to its strong correlation with the width of the profile.

As for the spread in Brillouin frequencies due to the finite acceptance angle, we recall that the Brillouin-frequency shift ν is related to the acoustic-phonon phase velocity v through

$$\nu=\frac{v}{\lambda_0}(n_i^2+n_s^2-2n_in_s\cos\theta)^{1/2}\ , \tag{1}$$

with θ the scattering angle *inside* the crystal, λ_0 the laser wavelength in vacuum, and n_i and n_s the refractive indices for the incident and scattered light. In the present setup, the detected beam is limited to a circular cross section, providing an acceptance angle as small as 1.4°. Thus, the scattering angle *outside* the crystal, θ_e, extends to 0.7° to either side of the median scattering condition ($\theta=\theta_e=90°$), with a weight which to very good approximation varies with θ_e according to a semicircle. To convert this to frequencies, we use that in the case of 90°

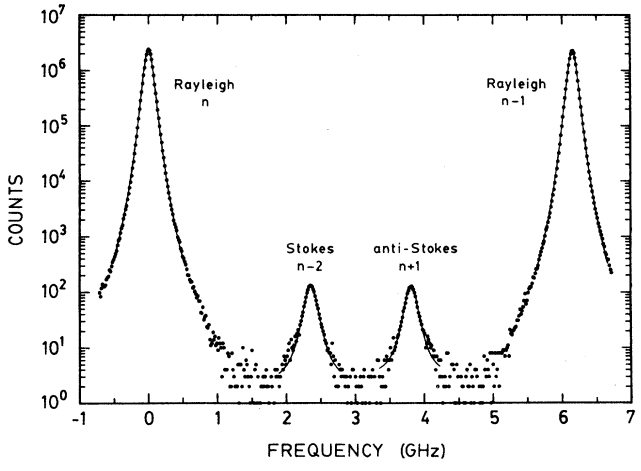

FIG. 1. Brillouin spectrum of C_{22}-mode L acoustic phonons in Rb_2ZnBr_4 at 333 K. Lines belong to different orders of the interferometer transmission, as indicated. The free spectral range is 6.155 GHz. Solid curves are fits, as discussed in text. Counting time per channel totals 1.12 s. The channel dwell time has been increased 20-fold in the passages through the Stokes and anti-Stokes lines, with corresponding scaling down of the channel contents.

scattering a departure of θ_e by $\delta\theta_e$ affects ν linearly by the amount

$$\delta\nu=\nu[n_i/(n_i^2+n_s^2)]\delta\theta_e$$

[cf. Eq. (1)]. Here, the angular dispersions of v, n_i, and n_s are ignored, but account is taken of the refraction at the sample surface, i.e., $\delta\theta_e/\delta\theta=n_s$. For longitudinal phonons in Rb_2ZnBr_4 ($n_i\approx n_s\approx 1.67$), for example, the distribution of Brillouin frequencies due to the scattering geometry alone is thus given by the analytic form $(\delta\nu_{\max}^2-\delta\nu^2)^{1/2}$ with $\delta\nu_{\max}=40$ MHz. As already noted, this distribution is to be convoluted with the bare instrumental profile to obtain an effective instrumental profile. This results in corrections of approximately 25–35 MHz in the phonon-induced broadening, compared to an instrumental width of 63 MHz. As concerns the neglect of the angular dispersions, detailed numerical calculations indicate that they may be entirely disregarded for phonons traveling along the crystal axes, and for other geometries have effects that are at least an order of magnitude smaller than $\delta\nu$.

The refractive indices of Rb_2ZnBr_4, necessary to extract the elastic constants from the Brillouin frequencies, have been measured at room temperature and $\lambda_0=514.5$ nm by use of a minimum deviation method with toluene as an immersion fluid. The results are $n_a=1.672\pm0.003$, $n_b=1.663\pm0.003$, and $n_c=1.680\pm0.003$, from which n_i and n_s may be derived. Literature values are available for the refractive indices of Rb_2ZnCl_4.[16]

III. RESULTS

A. Elastic constants

To determine the elastic constants of Rb_2ZnBr_4 at 300 K, Brillouin shifts have been measured for a selection of scattering geometries. The results are tabulated in Table I, together with the expressions for $\rho_m v^2$ connected with each mode observed. It is noted that these expressions are approximations for geometries for which the incident and detected light beams differ in their polarizations. In these cases, the phonon wave vector is not precisely aligned along the bisectrix of the photon wave vectors because of the finite anisotropy of the refraction, but numerical calculations indicate the departures not to exceed 0.3° and to have effects significantly below the experimental precision. The elastic constants have been deduced from the measured frequencies by fitting Eq. (1) with the expressions for $\rho_m v^2$ specified in Table I inserted. The mass density ρ_m is taken to be 3.683×10^3 kg/m^3. The results are, in GPa,

$$C_{11}=17.07\pm0.16\ ,$$
$$C_{22}=17.54\pm0.16\ ,$$
$$C_{33}=22.63\pm0.19\ ,$$
$$C_{44}=4.73\pm0.04\ ,$$
$$C_{55}=5.13+0.07\ ,$$
$$C_{66}=3.41\pm0.07\ ,$$
$$C_{12}=7.85\pm0.13\ ,$$
$$C_{13}=8.70\pm0.16\ ,$$
$$C_{23}=8.30\pm0.15\ .$$

Here, the uncertainties correspond to one standard deviation. The present results differ from those from ultrasonic experiments[25] by on the average 4% to either side. There is no apparent cause for the differences, but it is noted that in the latter case the crystals were, as distinct from the present ones, grown from an aqueous solution. Figure 2 shows the angular dispersion of the near-zone-center acoustic-phonon phase velocity, as calculated from the elastic constants just found. Note that the a and b axes are nearly identical as far as the elastic behavior is concerned.

In a similar way we have determined the elastic con-

TABLE I. Scattering geometries and observed Brillouin frequency shifts used in the determination of the elastic constants of Rb_2ZnBr_4 at 300 K. L, QL, T, and QT denote longitudinal, quasilongitudinal, transverse, and quasitransverse acoustic modes, respectively.

Scattering geometry	ν_{obs} (GHz)	Mode	$\rho_m v^2$
$xy(z,z)\bar{x}y$	9.956	L	C_{11}
$x\bar{y}(z,z)xy$	10.077	L	C_{22}
$xz(y,y)x\bar{z}$	11.325	L	C_{33}
$xz(y,xz)x\bar{z}$	5.225	T	C_{44}
$y(z,z)x$	9.606	QL	$\frac{1}{4}\{C_{11}+C_{22}+2C_{66}+[(C_{11}-C_{22})^2+4(C_{12}+C_{66})^2]^{1/2}\}$
	5.230	QT	$\frac{1}{4}\{C_{11}+C_{22}+2C_{66}-[(C_{11}-C_{22})^2+4(C_{12}+C_{66})^2]^{1/2}\}$
$y(z,y)x$	5.286	T	$\frac{1}{2}(C_{44}+C_{55})$
$z(x,x)y$	10.472	QL	$\frac{1}{4}\{C_{22}+C_{33}+2C_{44}+[(C_{22}-C_{33})^2+4(C_{23}+C_{44})^2]^{1/2}\}$
	5.756	QT	$\frac{1}{4}\{C_{22}+C_{33}+2C_{44}-[(C_{22}-C_{33})^2+4(C_{23}+C_{44})^2]^{1/2}\}$
$z(x,z)y$	4.988	T	$\frac{1}{2}(C_{55}+C_{66})$
$z(y,y)x$	10.516	QL	$\frac{1}{4}\{C_{11}+C_{33}+2C_{55}+[(C_{11}-C_{33})^2+4(C_{13}+C_{55})^2]^{1/2}\}$
	5.554	QT	$\frac{1}{4}\{C_{11}+C_{33}+2C_{55}-[(C_{11}-C_{33})^2+4(C_{13}+C_{55})^2]^{1/2}\}$
$z(y,z)x$	4.811	T	$\frac{1}{2}(C_{44}+C_{66})$

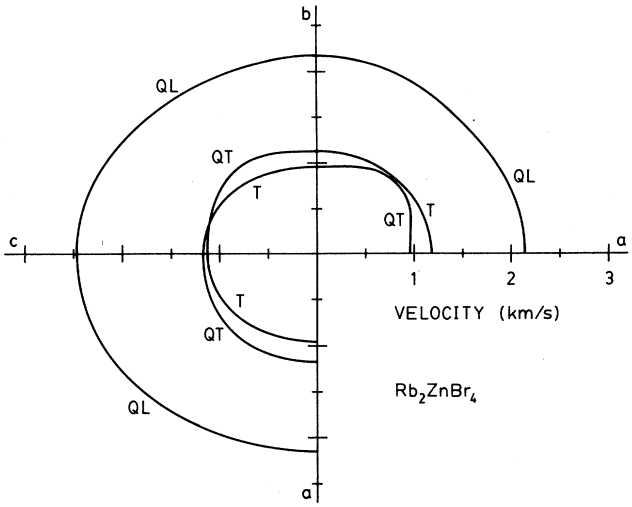

FIG. 2. Polar diagram of the acoustic-phonon phase velocity in Rb_2ZnBr_4, as calculated from measured elastic constants at 300 K. Quasilongitudinal, quasitransverse, and transverse phonon modes are indicated by QL, QT, and T, respectively. On the axes the QL modes turn strictly longitudinal.

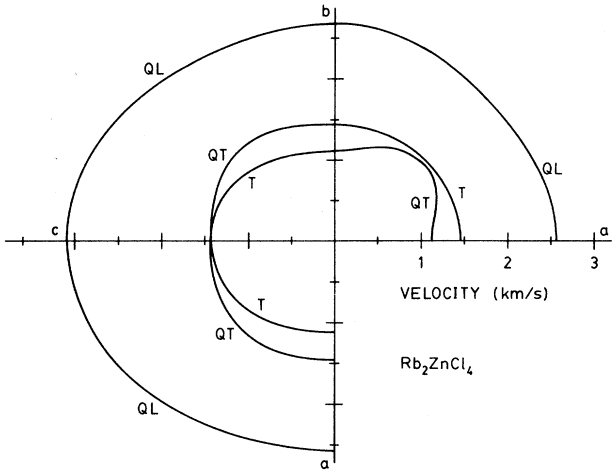

FIG. 3. As Fig. 2, but for Rb_2ZnCl_4.

stants of Rb_2ZnCl_4. The results are, in GPa,

$$C_{11}=19.27\pm0.19\ ,$$
$$C_{22}=20.96\pm0.19\ ,$$
$$C_{33}=28.2\pm0.5\ ,$$
$$C_{44}=6.10\pm0.05\ ,$$
$$C_{55}=6.22\pm0.05\ ,$$
$$C_{66}=3.67\pm0.08\ ,$$
$$C_{12}=8.53\pm0.14\ ,$$
$$C_{13}=9.2\pm0.6\ ,$$
$$C_{23}=9.4\pm0.2\ .$$

These values coincide within errors with those found by Luspin *et al.*,[16] yet are slightly more accurate. Figure 3, then, gives the calculated angular dispersion of the acoustic-phonon phase velocity for Rb_2ZnCl_4.

B. Temperature dependence of Brillouin spectra

Figures 4 and 5 show the variation of the Brillouin shift and the linewidth of longitudinal-acoustic phonons in Rb_2ZnBr_4 in the temperature range of 55 to 380 K. It is noted that the data are the less accurate the lower the temperature because of the associated reduction of the scattered light intensity. All data were taken on heating runs. The most distinctive features are as the following: (i) In an interval of about 20 K around the normal-to-incommensurate (N-I) transition at $T_1\approx353$ K, the C_{11} discerned in the linewidth data (Fig. 5). The data of the C_{33} mode, on the other hand, do not reveal a significant anomaly near T_1. (ii) At the incommensurate-to-commensurate (I-C) transition at $T_2\approx194$ K, a small but distinct step is apparent in the Brillouin frequency of the C_{11} mode, but absent from the frequencies of the C_{22} and

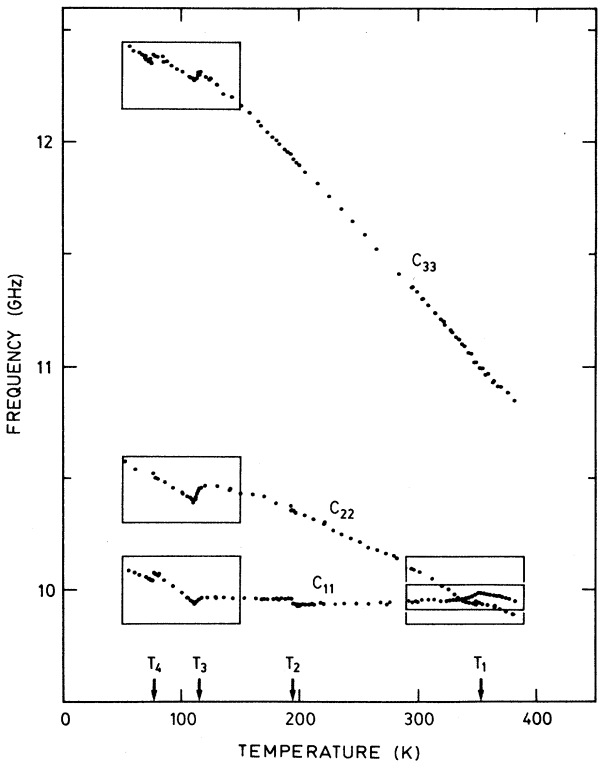

FIG. 4. Brillouin frequency shifts vs the temperature of C_{11}-, C_{22}-, and C_{33}-mode L acoustic phonons in Rb_2ZnBr_4, as measured in the scattering geometries specified in Table I. Enlargements around T_1, T_3, and T_4 are presented in Figs. 7 and 8.

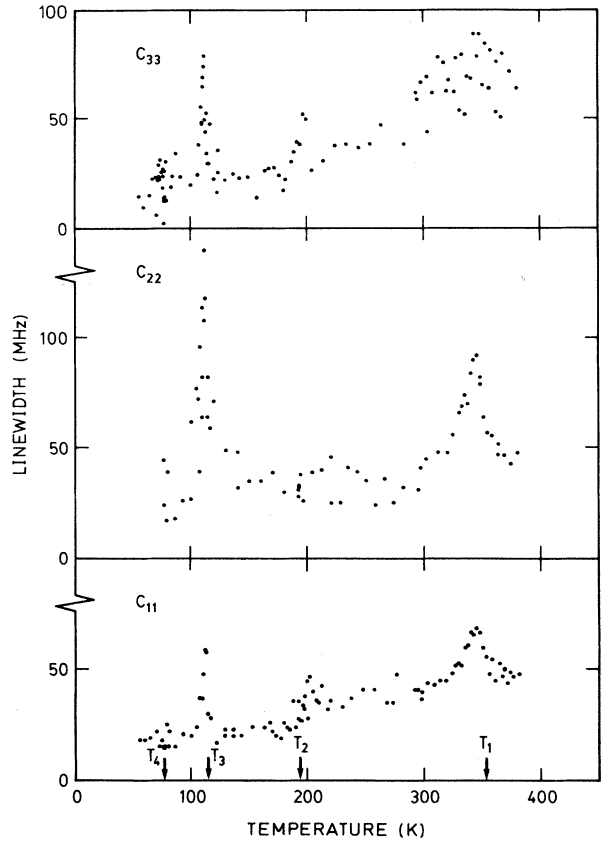

FIG. 5. Linewidths (FWHM) vs the temperature for C_{11}-, C_{22}-, and C_{33}- mode L acoustic phonons in Rb_2ZnBr_4.

and C_{22} modes behave anomalously. This is most clearly discerned in the linewidth data (Fig. 5). The data of the C_{33} mode, on the other hand, do not reveal a significant anomaly near T_1. (ii) At the incommensurate-to-commensurate (I-C) transition at $T_2 \approx 194$ K, a small but distinct step is apparent in the Brillouin frequency of the C_{11} mode, but absent from the frequencies of the C_{22} and C_{33} modes. The C_{11} and C_{33} modes tend to show a slightly enhanced linewidth near T_2. (iii) At lower temperatures, anomalies in the Brillouin frequency are observed just below $T_3 \approx 115$ K and at $T_4 \approx 76$ K. The anomaly near T_3, which extends over a temperature interval of about 5 K, is accompanied with a substantial enhancement of the linewidth for all three directions. The anomaly at T_4 involves distinct steps in the frequencies of the C_{11} and C_{33} modes, without any measurable effects on the linewidth.

IV. ACOUSTIC ANOMALIES

To derive explicit expressions for the anomalous elastic constants and the damping of the acoustic modes due to interaction with the soft-going mode, we resort to the approach of Levanyuk[18] and Yao *et al.*[19] This method allows us to relate the elastic susceptibility to the order parameter as well as its fluctuations, the latter of which of course corresponds to the amplitudons and phasons in the incommensurate regime. The calculation is conducted by use of the Lagrange formalism in a classical continuum approximation, with inclusion of the interaction of the acoustic and soft-going modes. First, a set of coupled equations of motion is derived for the soft-phonon coordinates and the strain, with the latter restricted to longitudinal-acoustic ones. For the incommensurate regime, these equations are subsequently rewritten to amplitudon, phason, and strain variables, with the order parameter occurring explicitly. After linearization for small strains and application of the fluctuation-dissipation theorem, an expression is then deduced for the linear elastic susceptibility up to second order in the order parameter fluctuations. Both the first- and second-order contributions appear to affect the frequency and damping of the acoustic modes as measured with Brillouin scattering.

We first consider the static modulation and the static uniform strains resulting from it. The internal energy density appropriate for β-K_2SO_4-type crystals may be expanded in the soft-phonon complex coordinate $Q(\mathbf{q}=\mathbf{0})$ and the strains e_i of the acoustical waves, to read[20]

$$U=\tfrac{1}{2}AQQ^*+\tfrac{1}{4}B(QQ^*)^2+\tfrac{1}{2}\sum_{i,j=1}^{3}C_{ij}^0e_ie_j+\tfrac{1}{2}\sum_{i=4}^{6}C_{ii}^0e_i^2+\sum_{i=1}^{3}g_ie_iQQ^*+\left[\sum_{i,j=1}^{3}h_{ij}e_ie_j+\sum_{i=4}^{6}h_{ii}e_i^2\right]QQ^* . \tag{2}$$

Here, the coefficient A is taken proportional to $T-T_i$. The first two terms are the leading terms in the Landau expansion, giving rise to a second-order phase transition at T_i. The next two terms, in which the C_{ij}^0 are the elastic constants unperturbed by the soft mode, represent the elastic energy. The remaining terms finally represent the lowest-order nonlinear interaction between the strains and pairs of soft phonons allowed by the relevant space group $Pmcn$.[20] It is noted that the fourth-order h terms, although in the present systems escaping determination (cf. Sec. V), have below been carried through, with the exception of Eqs. (4) and (5).

Upon defining $QQ^*=\rho^2$, the order parameter $\rho_0=\langle\rho\rangle$ and the static strains e_{0i} follow from the minimum energy conditions $\partial U/\partial\rho=0$ and $\partial U/\partial e_i=0$, which yield

$$A+B\rho_0^2+2\sum_{i=1}^{3}g_ie_{0i}+2\sum_{i,j=1}^{3}h_{ij}e_{0i}e_{0j}+2\sum_{i=4}^{6}h_{ii}e_{0i}^2=0 , \tag{3a}$$

$$\sum_{j=1}^{3}(C_{ij}^0+2h_{ij}\rho_0^2)e_{0j}=-g_i\rho_0^2 \quad (i=1,2,3) , \tag{3b}$$

and $e_{0i}=0$ $(i=4,5,6)$. The only nonzero static strains thus are the longitudinal ones e_{01}, e_{02}, and e_{03}. They are given by

$$e_{0i}=-\sum_{j=1}^{3}(C^0)_{ij}^{-1}g_j\rho_0^2 \quad (i=1,2,3) . \tag{4}$$

Using this result, we have for the order parameter below T_i

$$\rho_0^2 = -A \Big/ \left[B - 2 \sum_{i,j=1}^{3} (C^0)_{ij}^{-1} g_i g_j \right] . \tag{5}$$

Equations (4) and (5) are to lowest order in the order parameter, which amounts to neglect of the h terms.

For a calculation of the dynamical properties, the internal energy density, Eq. (2), needs to be supplemented with a gradient term of the form $\sum_i D_i (\partial Q/\partial x_i)(\partial Q^*/\partial x_i)$, describing the soft-mode dispersion.[12] To make the calculation tractable, we limit ourselves to longitudinal-acoustic phonons traveling along the crystal axes, simplifying Eq. (2) in its strain dependency. Upon writing $Q = \rho e^{-i\phi}$, with ρ and ϕ dependent on space and time, the potential energy density is then given by

$$U = \tfrac{1}{2} A\rho^2 + \tfrac{1}{4} B\rho^4 + \tfrac{1}{2} \sum_{i=1}^{3} D_i \left[\left(\frac{\partial \rho}{\partial x_i} \right)^2 + \rho^2 \left(\frac{\partial \phi}{\partial x_i} \right)^2 \right] + \tfrac{1}{2} \sum_{i=1}^{3} C_{ii}^0 e_i^2 + \sum_{i=1}^{3} g_i e_i \rho^2 + \sum_{i,j=1}^{3} h_{ij} e_i e_j \rho^2 . \tag{6}$$

The kinetic energy density similarly reads[12]

$$T = \tfrac{1}{2} \mu \dot{Q} \dot{Q}^* + \tfrac{1}{2} \rho_m \sum_{i=1}^{3} \dot{u}_i^2 = \tfrac{1}{2} \mu (\dot{\rho}^2 + \rho^2 \dot{\phi}^2) + \tfrac{1}{2} \rho_m \sum_{i=1}^{3} \dot{u}_i^2 , \tag{7}$$

in which μ is the effective mass density for the soft mode, ρ_m is the mass density, and $u_i(\mathbf{r})$ are displacements in the x_i direction, related to the longitudinal elastic strains by $e_i = \partial u_i/\partial x_i$. To probe the fluctuations, fictitious external driving forces are included by adding to the potential energy density

$$U_{\text{ext}} = -\sum_{i=1}^{3} \sigma_i e_i - \rho f_\rho - \rho\phi f_\phi , \tag{8}$$

in which σ_i is the driving stress associated with the strain e_i, and f_ρ and f_ϕ are the driving forces for the fluctuations of the amplitude and phase of the soft mode. Finally, damping is included in a phenomenological way by means of a Rayleigh dissipation function of the form

$$F = \tfrac{1}{2} \mu \Gamma (\dot{\rho}^2 + \rho^2 \dot{\phi}^2) + \tfrac{1}{2} \rho_m \sum_{i=1}^{3} \gamma_i \dot{e}_i^2 , \tag{9}$$

in which Γ denotes the damping of the soft mode, while the last term represents a wave-vector-dependent damping of magnitude $\gamma_i q_i^2$ of the C_{ii}-mode acoustic phonon.

The equations of motion for ρ, ϕ, and e_i are subsequently obtained from the Lagrange formalism for continuous systems,

$$L = T - U - U_{\text{ext}} ,$$

$$\frac{d}{dt} \frac{\partial L}{\partial \dot{\Psi}} + \sum_{i=1}^{3} \frac{\partial}{\partial x_i} \frac{\partial L}{\partial (\partial \Psi/\partial x_i)} - \frac{\partial L}{\partial \Psi} + \frac{\partial F}{\partial \dot{\Psi}} - \sum_{i=1}^{3} \frac{\partial}{\partial x_i} \frac{\partial F}{\partial (\partial \dot{\Psi}/\partial x_i)} = 0 , \tag{10}$$

in which the field variable Ψ is to be identified with ρ, ϕ, or u_i. After taking the derivatives of the equations for u_i with respect to x_i, the space-time Fourier transforms of the equations of motion for ρ, ϕ, and e_i become

$$\left[-\mu\Omega^2 - i\mu\Gamma\Omega + \sum_{i=1}^{3} D_i q_i^2 \right] \rho(\mathbf{q},\Omega) + \mu \{ \rho * \Omega\phi * \Omega\phi \}_{\mathbf{q},\Omega} + A\rho(\mathbf{q},\Omega) + B\{\rho*\rho*\rho\}_{\mathbf{q},\Omega} - \sum_{i=1}^{3} D_i \{\rho * q_i\phi * q_i\phi\}_{\mathbf{q},\Omega} + 2\sum_{i=1}^{3} g_i \{e_i * \rho\}_{\mathbf{q},\Omega} + 2\sum_{i,j=1}^{3} h_{ij} \{e_i * e_j * \rho\}_{\mathbf{q},\Omega} = f_\rho(\mathbf{q},\Omega) + \{\phi * f_\phi\}_{\mathbf{q},\Omega} , \tag{11a}$$

$$(-\mu\Omega - i\mu\Gamma)\{\rho*\rho*\Omega\phi\}_{\mathbf{q},\Omega} + \sum_{i=1}^{3} D_i q_i \{\rho*\rho*q_i\phi\}_{\mathbf{q},\Omega} = \{\rho * f_\phi\}_{\mathbf{q},\Omega} , \tag{11b}$$

$$(-\rho_m\omega^2 - i\rho_m\gamma_i k_i^2\omega + C_{ii}^0 k_i^2) e_i(\mathbf{k},\omega) + g_i k_i^2 \{\rho*\rho\}_{\mathbf{k},\omega} + 2\sum_{j=1}^{3} h_{ij} k_i^2 \{e_j*\rho*\rho\}_{\mathbf{k},\omega} = k_i^2 \sigma(\mathbf{k},\omega) , \tag{11c}$$

where the symbols $\{\ *\ \}$ and $\{\ *\ *\ \}$ denote convolutions of the functions within, $\mathbf{q}$ and Ω are the soft-mode wave vector and angular frequency, and the corresponding quantities of the acoustic wave are, for clarity, denoted by $\mathbf{k}$ and ω.

We first apply Eqs. (11) to the incommensurate regime, in which both the amplitude and the phase of Q may fluctuate. To separate out these fluctuations and those of the strains about the equilibrium values ρ_0, ϕ_0, and e_{0i}, we set

$$\begin{aligned} \rho(\mathbf{q},\Omega) &= \rho_0 \delta(\mathbf{q})\delta(\Omega) + P_A(\mathbf{q},\Omega)/2^{1/2} , \\ \phi(\mathbf{q},\Omega) &= \phi_0 \delta(\mathbf{q})\delta(\Omega) - P_\phi(\mathbf{q},\Omega)/2^{1/2}\rho_0 , \\ e_i(\mathbf{k},\omega) &= e_{0i}\delta(\mathbf{k})\delta(\omega) + \delta e_i(\mathbf{k},\omega) , \end{aligned} \tag{12}$$

where, following Bruce and Cowley,[26] we have introduced the amplitudon and the phason coordinates

$$\begin{aligned} P_A &= (\delta Q^* e^{-i\phi_0} + \delta Q e^{i\phi_0})/2^{1/2} , \\ P_\phi &= i(\delta Q^* e^{-i\phi_0} - \delta Q e^{i\phi_0})/2^{1/2} . \end{aligned} \tag{13}$$

Substituting Eqs. (12) into Eqs. (11) and eliminating the static terms by use of Eq. (3), we find for the equations of motion of the amplitudons, the phasons, and the longitudinal-acoustic waves

$$P_A(\mathbf{q},\Omega) = \chi_A^0(\mathbf{q},\Omega) f_A(\mathbf{q},\Omega) - 2^{3/2}\chi_A^0(\mathbf{q},\Omega) \sum_{i=1}^{3} g_i' \rho_0 \delta e_i(\mathbf{q},\Omega) - 2\chi_A^0(\mathbf{q},\Omega) \sum_{i=1}^{3} g_i' \{\delta e_i * P_A\}_{\mathbf{q},\Omega} , \tag{14a}$$

$$P_\phi(\mathbf{q},\Omega) = \chi_\phi^0(\mathbf{q},\Omega) f_\phi'(\mathbf{q},\Omega) , \tag{14b}$$

$$\sigma_i(\mathbf{k},\omega)=\frac{1}{\chi^0_{e_i}(\mathbf{k},\omega)}\delta e_i(\mathbf{k},\omega)+2h_{ii}\rho_0^2\delta e_i(\mathbf{k},\omega)$$
$$+2^{1/2}g_i'\rho_0 P_A(\mathbf{k},\omega)+\tfrac{1}{2}g_i'\{P_A*P_A\}_{\mathbf{k},\omega}$$
$$+2^{3/2}h_{ii}\rho_0\{\delta e_i*P_A\}_{\mathbf{k},\omega}\ , \tag{14c}$$

where

$$f_A(\mathbf{q},\Omega)=2^{1/2}f_\rho(\mathbf{q},\Omega)\ ,$$
$$f'_\phi(\mathbf{q},\Omega)=-2^{1/2}f_\phi(\mathbf{q},\Omega)\ ,$$

and the g_i are renormalized by the static strains, Eq. (4), according to

$$g_i'=g_i+2\sum_{j=1}^{3}h_{ij}e_{0j}\ . \tag{15}$$

We note that Eqs. (14) have been linearized in δe_i. Further, in Eqs. (14a) and (14b) terms in P_A and P_ϕ of order higher than the first are discarded. In Eq. (14c), however, terms of second order in P_A are kept, enabling us to calculate the second-order effect of the order-parameter fluctuations on the elastic behavior. As is seen from Eq. (14b), the phasons do not interact with the strains within the assumptions underlying Eq. (2). The susceptibilities entering Eqs. (14) are those in the absence of interaction, as is indicated with the superscript 0. They have the standard form of the susceptibility of a damped harmonic oscillator, and are given by

$$\chi^0_A(\mathbf{q},\Omega)=1/\mu[\Omega_A^2(\mathbf{q})-\Omega^2-i\Gamma\Omega]\ , \tag{16a}$$
$$\chi^0_\phi(\mathbf{q},\Omega)=1/\mu[\Omega_\phi^2(\mathbf{q})-\Omega^2-i\Gamma\Omega]\ , \tag{16b}$$
$$\chi^0_{e_i}(\mathbf{k},\omega)=1/(\rho_m/k_i^2)[(k_i^2/\rho_m)C^0_{ii}-\omega^2-i\gamma_i k_i^2\omega]\ , \tag{16c}$$

with the dispersion relations, in circular frequencies,

$$\Omega_A^2(\mathbf{q})=\frac{1}{\mu}\left[2B\rho_0^2+\sum_{i=1}^{3}D_iq_i^2\right]\ ,$$
$$\Omega_\phi^2(\mathbf{q})=\frac{1}{\mu}\sum_{i=1}^{3}D_iq_i^2\ . \tag{17}$$

We note that the amplitudon susceptibility has been derived by use of the condition for static equilibrium Eq. (3a). The frequencies of the phasons do not contain ρ_0 and vanish at $\mathbf{q}=\mathbf{0}$, reflecting their independence of the phase of the modulation wave. As the damping is finite, the phasons are overdamped for small wave vectors. The amplitudons do not become overdamped until approaching T_i, where their frequency vanishes.

We proceed with deriving the effect of the amplitudons on the elastic susceptibilities associated with the longitudinal-acoustic phonons. To this end, we substitute Eq. (14a) into Eq. (14c). As we are concerned with the linear susceptibilities, only terms linear in δe_i need be considered, which has been anticipated in Eqs. (14). Further, after averaging over the order-parameter fluctuations, only terms of order even in P_A^0 remain. Noting that the amplitudon coordinate in the absence of coupling equals

$$P_A^0(\mathbf{q},\Omega)=\chi_A^0(\mathbf{q},\Omega)f_A(\mathbf{q},\Omega)\ , \tag{18}$$

we have

$$\langle\sigma_i(\mathbf{k},\omega)\rangle=\frac{1}{\chi^0_{e_i}(\mathbf{k},\omega)}\delta e_i(\mathbf{k},\omega)+2h_{ii}\rho_0^2\delta e_i(\mathbf{k},\omega)$$
$$-4g_i'^2\rho_0^2\chi_A^0(\mathbf{k},\omega)\delta e_i(\mathbf{k},\omega)$$
$$-2g_i'^2\langle\{P_A^0*\chi_A^0\{\delta e_i*P_A^0\}\}_{\mathbf{k},\omega}\rangle\ . \tag{19}$$

The double convolution occurring in Eq. (19) is evaluated with the help of the fluctuation-dissipation theorem,

$$\langle P_A^0(\mathbf{q},\Omega)P_A^0(\mathbf{q}',\Omega')\rangle$$
$$=\frac{k_BT}{(2\pi)^4\Omega}\mathrm{Im}\chi_A^0(\mathbf{q},\Omega)\delta(\mathbf{q}+\mathbf{q}')\delta(\Omega+\Omega')\ , \tag{20}$$

to reduce to

$$\langle\{P_A^0*\chi_A^0\{\delta e_i*P_A^0\}\}_{\mathbf{k},\omega}\rangle=\frac{k_BT}{(2\pi)^4}\delta e_i(\mathbf{k},\omega)I_A(\mathbf{k},\omega)\ , \tag{21}$$

with

$$I_A(\mathbf{k},\omega)=\int\chi_A^0(\mathbf{k}-\mathbf{q},\omega-\Omega)\mathrm{Im}\chi_A^0(\mathbf{q},\Omega)\frac{d\Omega}{\Omega}d\mathbf{q}\ . \tag{22}$$

Below T_i, the elastic susceptibilities $\chi_{e_i}(\mathbf{k},\omega)=\delta e_i/\langle\sigma_i(\mathbf{k},\omega)\rangle$ then are given by

$$\frac{1}{\chi_{e_i}(\mathbf{k},\omega)}=\frac{1}{\chi^0_{e_i}(\mathbf{k},\omega)}+2h_{ii}\rho_0^2-4g_i'^2\rho_0^2\chi_A^0(\mathbf{k},\omega)$$
$$-2g_i'^2\frac{k_BT}{(2\pi)^4}I_A(\mathbf{k},\omega)\ . \tag{23}$$

Equation (23) constitutes the final result of the present Landau theory. The second term on the right-hand side of Eq. (23) is the lowest-order contribution resulting from the h part of the interaction in Eq. (2), which is quadratic in both the order parameter and the strains. The third and fourth terms primarily arise from the g part of the interaction, which is quadratic in the order parameter, but linear in the strains [cf. Eq. (15)]. The fluctuations being separated out according to Eq. (12), the third term represents an effective bilinear coupling of the strain fluctuations and the order-parameter fluctuations. Induced by the static order parameter, it vanishes above T_i. Similarly, the fourth term provides a coupling linear in the strain but quadratic in the order-parameter fluctuations. It contributes at both sides of T_i, and is referred to as the fluctuation term.

We proceed with bringing Eq. (23) into a form that allows comparison with experiment. The amplitudon susceptibility, Eq. (16a), is substituted into the fluctuation integral $I_A(\mathbf{k},\omega)$ while making the approximation $\chi_A^0(\mathbf{k}-\mathbf{q},\omega-\Omega)=\chi_A^0(-\mathbf{q},\omega-\Omega)$, which is correct for $\omega/\Gamma\ll1$. (In the present systems $\omega/\Gamma<0.1$; cf. Sec. V.) The integration over Ω can then be carried out straightforwardly by contour integration, yielding

$$I_A(\mathbf{k},\omega)=\frac{2\pi}{\mu^2}\int\frac{(1-i\omega/2\Gamma)d\mathbf{q}}{(1-i\omega/\Gamma)\Omega_A^2(\mathbf{q})[4\Omega_A^2(\mathbf{q})-2i\omega\Gamma(1-i\omega/2\Gamma)]}\ . \tag{24}$$

Neglecting terms of order ω/Γ in Eq. (24), and integrating over the wave vector, we find

$$I_A(\mathbf{k},\omega)=\frac{2\pi^3 i}{\mu^{1/2}D^{3/2}\omega\Gamma}\{[\Omega_A^2(\mathbf{0})-\tfrac{1}{2}i\omega\Gamma]^{1/2}-\Omega_A(\mathbf{0})\}\ , \tag{25}$$

with $D^{3/2}$ standing for $(D_1D_2D_3)^{1/2}$. In the third, bilinear, term on the right-hand side of Eq. (23), we further approximate $\Omega_A^2(\mathbf{k})-\omega^2$ in $\chi_A^0(\mathbf{k},\omega)$ to $\Omega_A^2(0)$ to obtain $\chi_A^0(\mathbf{k},\omega)=[\mu(\Omega_A^2(\mathbf{0})-i\omega\Gamma)]^{-1}$. Within these approximations, the elastic constant C_{ii} and the damping Γ_i of longitudinal-acoustic phonons traveling along the x_i axis can, by comparison with Eq. (16c), finally be identified as

$$\begin{aligned}C_{ii}&=C_{ii}^0+2h_{ii}\rho_0^2+4\frac{g_i'^2\rho_0^2}{\mu\Omega_A^2(\mathbf{0})}\left[\frac{-1}{1+\omega^2\tau^2}\right]+\frac{g_i'^2k_BT}{4\pi\mu^{1/2}D^{3/2}(\omega\Gamma)^{1/2}}\left[\frac{-\{\frac{1}{2}[(1+\frac{1}{4}\omega^2\tau^2)^{1/2}-1]\}^{1/2}}{(\omega\tau)^{1/2}}\right],\\ \Gamma_i&=\gamma_ik_i^2+2\frac{k_i^2}{\rho_m}\frac{g_i'^2\rho_0^2}{\mu\omega\Omega_A^2(\mathbf{0})}\left[\frac{2\omega\tau}{1+\omega^2\tau^2}\right]+\frac{k_i^2}{\rho_m}\frac{g_i'^2k_BT}{8\pi\mu^{1/2}D^{3/2}\omega^{3/2}\Gamma^{1/2}}\left[\frac{\{2[(1+\frac{1}{4}\omega^2\tau^2)^{1/2}+1]\}^{1/2}-2}{(\omega\tau)^{1/2}}\right],\end{aligned} \tag{26}$$

with

$$\tau=\Gamma/\Omega_A^2(\mathbf{0})\ . \tag{27}$$

Figure 6 shows the $(\omega\tau)^{-1}$ dependences of the contributions to C_{ii} and Γ_i arising from the bilinear and fluctuation terms in Eq. (23), or rather, the functions contained within the large parentheses in Eq. (26). These functions are successively denoted by $F_n(\omega\tau)$, with $n=1$, 2, 3, and 4.

In the high-temperature phase, the equilibrium values ρ_0 and e_{0i} equal zero. The above description still holds, except that the mode the acoustic phonon couples with is the high-temperature soft mode rather than the amplitudon. By analogy with Eq. (23), we have

$$\frac{1}{\chi_{e_i}(\mathbf{k},\omega)}=\frac{1}{\chi_{e_i}^0(\mathbf{k},\omega)}-2g_i^2\frac{k_BT}{(2\pi)^4}I_S(\mathbf{k},\omega)\ , \tag{28}$$

from which integration yields

$$\begin{aligned}C_{ii}&=C_{ii}^0+\frac{g_i^2k_BT}{4\pi\mu^{1/2}D^{3/2}(\omega\Gamma)^{1/2}}\left[\frac{-\{\frac{1}{2}[(1+\frac{1}{4}\omega^2\tau^2)^{1/2}-1]\}^{1/2}}{(\omega\tau)^{1/2}}\right],\\ \Gamma_i&=\gamma_ik_i^2+\frac{k_i^2}{\rho_m}\frac{g_i^2k_BT}{8\pi\mu^{1/2}D^{3/2}\omega^{3/2}\Gamma^{1/2}}\left[\frac{\{2[(1+\frac{1}{4}\omega^2\tau^2)^{1/2}+1]\}^{1/2}-2}{(\omega\tau)^{1/2}}\right],\end{aligned} \tag{29}$$

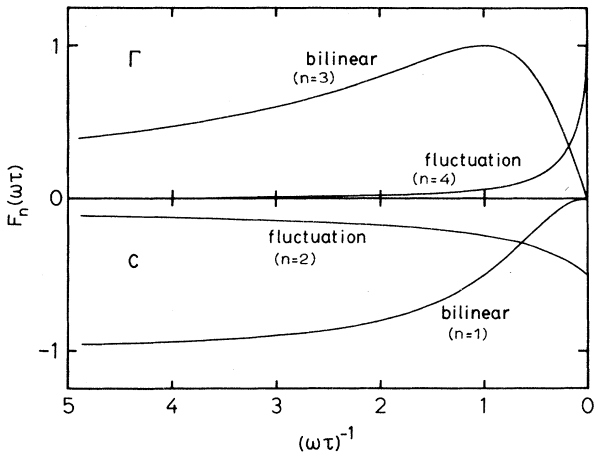

FIG. 6. Dependence of $(\omega\tau)^{-1}$ of the functions $F_n(\omega\tau)$ appearing within the large parentheses in Eqs. (26), representing the bilinear and fluctuation parts of C_{ii} and Γ_i. The parameter $(\omega\tau)^{-1}$ increases from right to left to facilitate comparison with experimental data below the transition, i.e., the point where $(\omega\tau)^{-1}$ vanishes.

with

$$\tau=\Gamma/\Omega_S^2(\mathbf{0})\ . \tag{30}$$

The dispersion relation of the high-temperature soft mode reads

$$\Omega_S^2(\mathbf{q})=\frac{1}{\mu}\left[A+\sum_{i=1}^{3}D_iq_i^2\right]\ . \tag{31}$$

V. DISCUSSION

The Brillouin scattering experiments provide the frequency shift ν_i and the full width at half maximum (FWHM) Δ_i invoked by phonons traveling at a given wave vector along the x_i axis. The anomalous parts $\delta\nu_i$ and $\delta\Delta_i$ of these quantities are related to the excess elastic constants and damping [cf. Eqs. (26) and (29)] by

$$\delta\nu_i=\frac{k_i^2}{4\pi\rho_m\omega}(C_{ii}-C_{ii}^0),\quad \delta\Delta_i=(\Gamma_i-\gamma_ik_i^2)/2\pi\ , \tag{32}$$

provided that, as is the case in our systems, the frequency anomaly is small relative to the phonon frequency. The nonanomalous parts ν_i^0 and Δ_i^0 are in turn given by

$$\nu_i^0=(2^{1/2}n_{i,s}/\lambda_0)(C_{ii}^0/\rho_m)^{1/2} ,$$

which follows by use of Eq. (1), and $\Delta_i^0=\gamma_i k_i^2/2\pi$. Note that in C_{ii} and Γ_i the prefactors to the functions $F_1(\omega\tau)$ and $F_3(\omega\tau)$ in the bilinear terms become equal upon conversion to frequencies, as do the prefactors to $F_2(\omega\tau)$ and $F_4(\omega\tau)$ in the fluctuation terms. After conversion to frequencies these prefactors are, respectively,

$$K_1=\frac{k_i^2 g_i'^2 \rho_0^2}{\pi\rho_m\mu\omega\Omega_A^2(0)} ,$$
$$K_2(T)=\frac{k_i^2 g_1'^2 k_B T}{16\pi^2\rho_m\mu^{1/2}D^{3/2}\omega^{3/2}\Gamma^{1/2}} . \quad (33)$$

A. Rb_2ZnBr_4 near the *N-I* transition

We first discuss the adjustment of the theoretical expressions for the frequency $\nu_i=\delta\nu_i+\nu_i^0$ and the linewidth $\Delta_i=\delta\Delta_i+\Delta_i^0$, i.e., Eqs. (32) with Eqs. (26) or Eqs. (29) inserted and augmented with the backgrounds, to coincide with the experimental data of Rb_2ZnBr_4 in the temperature regime around the *N-I* transition. The quantities to be fitted are the prefactors K_1 and K_2 of the bilinear and fluctuation terms, the transition temperature T_1, the relaxation time τ, and finally the backgrounds ν_i^0 and Δ_i^0. In the fits, all contributions arising from the fourth-order h terms are ignored, in particular the part $2h_{ii}\rho_0^2$ in C_{ii}. The rationale for doing so is that it proved impossible to discern a contribution in C_{ii} dependent on ρ_0^2, which below T_1 would go as $(T_1-T)^{2\beta}$ with $\beta=0.35$.[27] In this respect, therefore, K_2ZnBr_4 is notably different from the case of K_2SeO_4.[21–23] Second, the h terms apparently being small, they may very well be rivaled by nonlinear interactions quadratic in the strains with optical phonons other than the soft mode, which below T_1 similarly give rise to a temperature-dependent elastic susceptibility proportional to the static strain [cf. Eq. (5)]. All of these effects have, therefore, been stored in the background ν_i^0. At T_1, the latter is taken continuous in value, but not necessarily continuous in the first derivative. In fact, ν_i^0 appears to be adequately represented by polynomials in T of at most degree one above T_1, and of at most degree two below T_1. The background Δ_i^0 of the linewidth is assumed to be independent of the temperature over the range of the fits.

As to the other parameters, K_1 is taken to be independent of the temperature, which amounts to, first, the assumption that ρ_0^2 and $\Omega_A^2(0)$ have identical temperature dependences, as in the Landau approximation [cf. Eq. (17)], and, second, the neglect of the renormalizing h terms in the g interaction [cf. Eq. (15)]. The parameter K_2 is explicitly dependent on the temperature. Leaving this dependence in the expressions, we take $K_2(T_1)$, or rather $K_2(T_1)/K_1$, as the fitting parameter. Also dependent on the temperature is the relaxation time τ. Here we distinguish between the amplitudon relaxation below T_1 and the soft-mode relaxation above T_1, in both cases adopting the usual Landau $|T-T_1|^{-1}$ dependence. That is,

$$\tau(T)=\tau_{A,S}^* T_1/|T-T_1| . \quad (34)$$

It is noted that experimental verification of Eq. (34) is available in the incommensurate phase in the case of K_2SeO_4.[22,23] Although simple Landau theory predicts that $\tau_S^*=2\tau_A^*$ [cf. Eqs. (5), (17), (27), (30), and (31)], these parameters are fitted independently.

In the actual fitting, fits of excellent quality have been achieved simultaneously to the frequency and linewidth data of each mode. The output values for T_1, τ_A^*, τ_S^*, and $K_2(T_1)/K_1$ appear to coincide within errors. In the case of the C_{11} mode, the theory with the fitted parameters inserted is compared with the data in Fig. 7(a); for the C_{22} mode the comparison is made in Fig. 7(b). A noteworthy

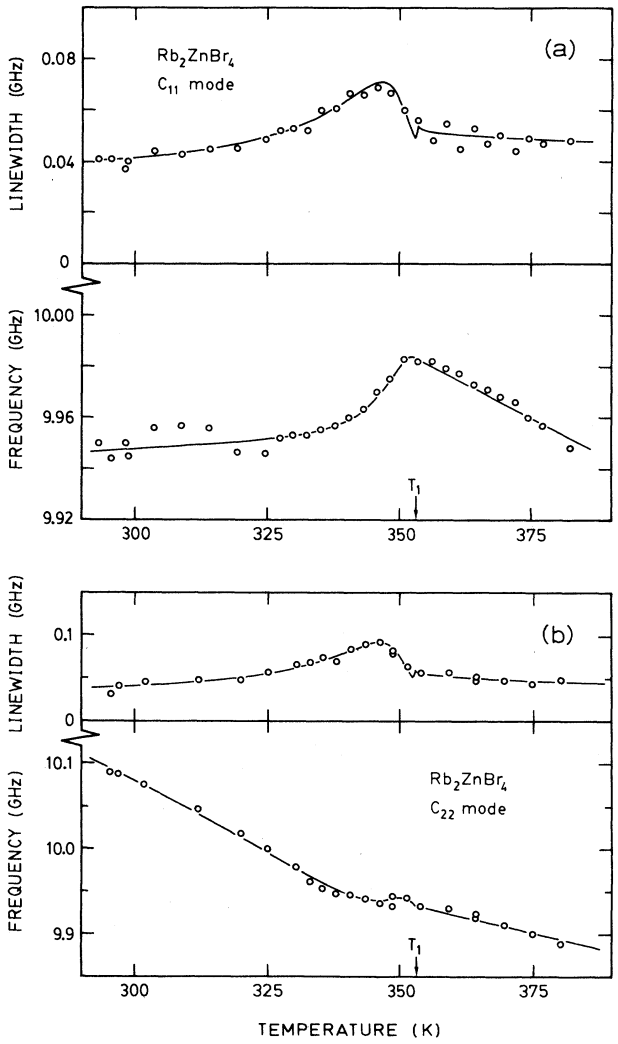

FIG. 7. Frequency and linewidth of (a) C_{11}-mode and (b) C_{22}-mode L acoustic phonons in Rb_2ZnBr_4 near T_1. Solid lines are simultaneous fits to the frequency and linewidth data.

conclusion deduced from these adjustments is, therefore, that the theory developed in Sec. IV is indeed capable of reproducing the anomalous parts of both the Brillouin frequencies and widths with a consistent set of parameters. The weighted averages of the output parameters are collected in Table II, as is K_1, which of course depends on the particular mode. It clearly is of interest to compare these results with those from other sources, and, whenever possible, with estimates derived from the theory. The present result for T_1 lies within the range of T_1's deduced from neutron scattering,[6] but deviates from the values around 347 K from dielectric,[2,8,28] x-ray,[7] and specific-heat[9] experiments. Of more interest are τ_A^* and τ_S^*. Another technique that allows probing of the amplitudon frequency and damping is Raman scattering. Raman experiments on Rb_2ZnBr_4 (Refs. 28–30) have been analyzed[31] to find for the width of the amplitudon, in our notation, $\Gamma/2\pi=13$ cm^{-1} at about 40 K below T_1, the closest distance at which the softening Raman line could be observed. At this point $\Omega_A/2\pi=10$ cm^{-1}, whence with Eq. (27) $\tau_A^*=8\times10^{-14}$ s, which is half an order smaller than our result. It should be emphasized, however, that our experiments have been performed closer to T_1, and therefore are likely to provide a more reliable estimate of the amplitudon relaxation just below the transition. As for the regime above the transition, the soft-mode parameters $\Gamma/2\pi$ and $\Omega_S/2\pi$ are available, although with considerable uncertainty, from an analysis of diffuse neutron scattering.[6] On the basis of a damped harmonic oscillator model, $\Gamma/2\pi$ has been found to be of order 0.1 THz around 200 °C, while $d(\Omega_S/2\pi)^2/dT \sim5\times10^{19}$ Hz^2/K. This leads to $\tau_S^*\sim10^{-12}$ s, which compared to our value is within the range of the combined uncertainties.

As concerns the prefactors of the bilinear and fluctuation parts, K_1 and K_2, it is feasible to compare them with estimates calculated from the theoretical expressions derived above. We first discuss the ratio $K_2(T_1)/K_1$, in which the coupling strength drops out. The experimental result $K_2(T_1)/K_1\approx0.6$ expresses that the bilinear and fluctuation parts of the acoustic anomalies are of comparable magnitude at Brillouin frequencies. To evaluate a theoretical estimate we first eliminate Ω_A by use of Eq. (27), to arrive at

$$K_2(T_1)/K_1=(k_BT_1/16\pi\rho_0^2\tau)(\mu\Gamma/D^3\omega)^{1/2}\ .$$

The combination $\rho_0^2\tau$ is supposedly independent of the temperature. The quantity τ is available from τ_A^* through Eq. (34). The order parameter ρ_0, which has not been determined directly in Rb_2ZnBr_4, may be estimated from the displacements in the incommensurate phase of the isostructural compound Rb_2ZnCl_4. Here, from EPR spectra of Mn^{2+} substituted for Zn^{2+},[27] the amplitude Q of the incommensurate rotation of the $ZnCl_4$ tetrahedra was found to vary with temperature just below T_1 according to $dQ^2/dT=-33$ deg^2/K, corresponding to $d\rho_0^2/dT=-2.5\times10^{-22}$ m^2/K. For the effective-mass density associated with the amplitudons we adopt $\mu\approx0.05\rho_m$ by analogy to K_2SeO_4,[32] for which μ may be derived from the stress dependence of the amplitudon frequency combined with thermal-expansion data. We have $\rho_m=3.68\times10^3$ kg/m^3. The damping Γ is taken from Raman data as above. For the amplitudon dispersion no data are available, but from a comparison with cases such as K_2SeO_4 (Ref. 33) it is not unreasonable to suppose that D/μ is of the order of the square of the transverse-acoustic phonon velocity. Accordingly, $D/\mu\approx1.2\times10^6$ m^2/s^2. Finally, $\omega=2\pi\times10$ GHz. Inserting these values, we find $K_2(T_1)/K_1\sim0.1$, which in view of the uncertainties of both the experiments and the parameters inserted into the theory is not incompatible with the result 0.6 from experiment.

Next, we turn to the absolute magnitude of the prefactors. We consider K_1 for the C_{11} and C_{22} modes, after first rewriting it as $k_i^2g_i'^2\rho_0^2\tau/\pi\rho_m\mu\omega\Gamma$. Of the quantities additional to the above, k_i is accurately known: $k_i=2.9\times10^7$ m^{-1}. This leaves us with the coupling coefficients $g_i'\approx g_i$, which are related to the anomalous thermal-expansion coefficients $\delta\alpha_i$ through the derivative of Eq. (4) with respect to the temperature, or $g_i=-\sum_j C_{ij}\delta\alpha_j/(d\rho_0^2/dT)$. Like $d\rho_0^2/dT$, estimated above, the quantities $\delta\alpha_i$ are not available for Rb_2ZnBr_4, but have been determined in Rb_2ZnCl_4.[34] Some caution should be exercised when inserting these results because the $\delta\alpha_i$ are of either sign, amplifying the uncertainties. We find $g_1=-7.8\times10^{26}$ kg/s^2 and $g_2=+1.3\times10^{27}$ kg/s^2, leading to $K_1=45$ MHz for the C_{11} mode and $K_1=124$ MHz for the C_{22} mode, again in consistency with experiment.

TABLE II. Output values of fits for the C_{11} and C_{22} modes in Rb_2ZnBr_4 near T_1.

τ_A^*	$(3.2\pm0.3)\times10^{-13}$ s
τ_S^*	$(3\pm2)\times10^{-11}$ s
T_1	353.1±0.7 K
$K_2(T_1)/K_1$	0.56±0.11
K_1 (C_{11} mode)	39±3 MHz
K_1 (C_{22} mode)	68±5 MHz

B. Low-temperature transitions of Rb_2ZnBr_4

In addition to the *N-I* transition at T_1, Rb_2ZnBr_4 undergoes a series of phase transitions at lower temperatures. Of these, the transition at $T_3\approx115$ K has previously been found to be of second order by specific-heat[9] experiments and nuclear quadrupole resonance (NQR).[10] Our data near T_3 show acoustic anomalies closely resembling those occurring near T_1. This not only lends support to the conclusion that the transition is of second order, but also suggests that the anomalies are caused by a similar mechanism, i.e., a coupling linear in the strain and quadratic in the coordinates of the soft mode associated with the transition. Assuming this to be the case, we have fitted the theoretical expressions for the frequency and the linewidth to the data for the C_{11}, C_{22}, and C_{33} modes around T_3 in a manner similar to the procedure outlined above for use near T_1. Here, $\tau_<^*$ and $\tau_>^*$ take the place of τ_A^* and τ_S^*, respectively. The results, presented

in Figs. 8(a)–8(c), are found to excellently track the data for all three modes considered. The fitted values of the K_1 of the three modes as well as the weighted averages of the results for T_3, $\tau^*_<$, $\tau^*_>$, and $K_2(T_3)/K_1$ are collected in Table III. Only for T_3 and $\tau^*_<$ a comparison with results from other sources is feasible. Values of T_3 extracted from x-ray,[7] dielectric,[3,11] specific-heat,[9] and NQR (Ref. 10) experiments range from 108 to 120 K, in accord with our result. The quantity $\tau^*_<$ is also derivable from Raman spectra. Below 90 K, a strongly temperature-dependent Raman mode has been observed,[29] which has been associated with the transition at T_3.[9] From the spectrum at 90 K, we have deduced the frequency $\Omega_</2\pi$ and the linewidth $\Gamma/2\pi$ of this mode, with the results ~ 8 and ~ 3 cm^{-1}, respectively. This leads to $\tau^*_< \sim 5\times 10^{-14}$ s, about half an order smaller than our finding.

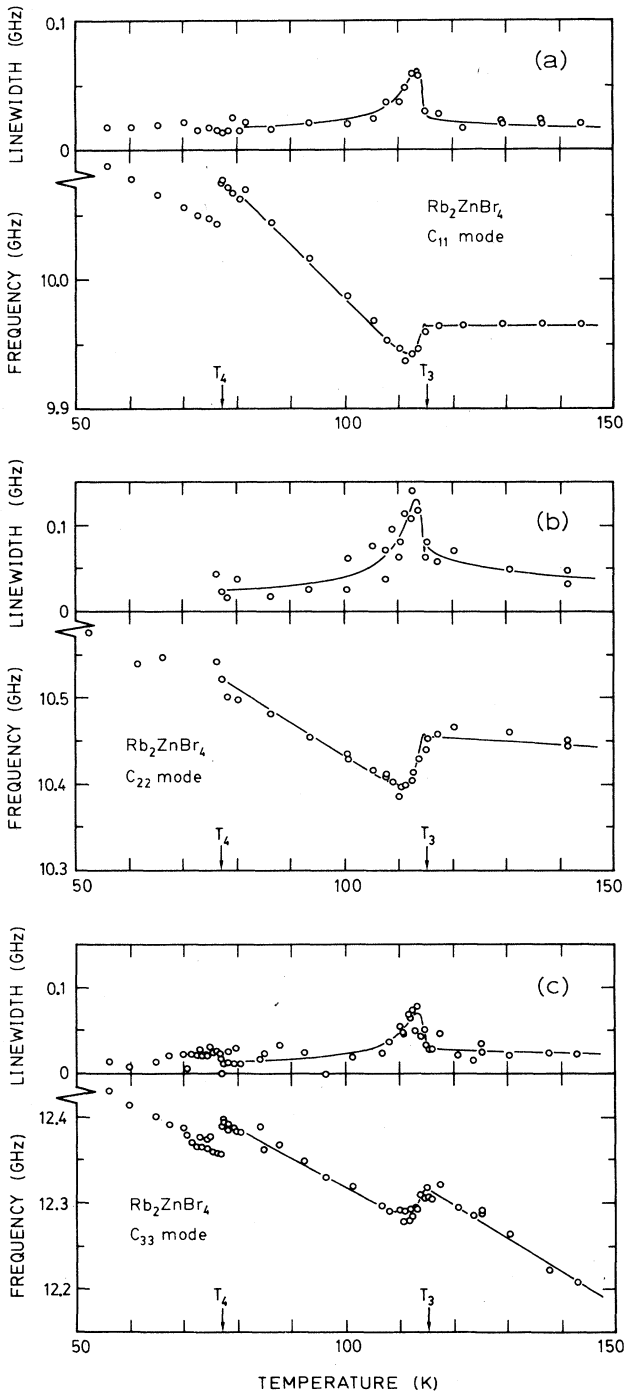

FIG. 8. Frequency and linewidth of (a) C_{11}-mode, (b) C_{22}-mode, and (c) C_{33}-mode L acoustic phonon in Rb_2ZnBr_4 near T_3 and T_4. Solid lines are fits.

In our experiments, the phase transitions at T_2 and T_4 are apparent by anomalies of a distinctly different nature. The transition from the incommensurate phase to the commensurate ferroelectric phase at T_2 is accompanied by a small step in the Brillouin frequency of the C_{11} mode (Fig. 4), presumably due to coupling of the strain with the spontaneous polarization below the transition. For the other modes no significant effects on the frequency are observed. The linewidth data (Fig. 5) are indicative of a small increase of the damping of the C_{11} and C_{33} modes just above the transition. Our result $T_2 = 193.8 \pm 0.8$ K is in good agreement with the results from dielectric[1,2,8,11,35] and specific-heat[9] measurements. The transition at T_4 is accompanied by small steps in the frequencies of the C_{11} and C_{33} modes, without noticeable effects on the linewidth. For the transition temperature we find $T_4 = 77.1 \pm 0.5$ K, while values found from x-ray,[7] dielectric,[3,11] and specific-heat[9] experiments range from 73 to 80 K.

C. Rb_2ZnCl_4 near T_1

The N-I transition in Rb_2ZnCl_4 has been investigated earlier with the technique of Brillouin spectroscopy by several authors. Luspin *et al.*[16] have reported on the temperature dependence of the elastic constants C_{11} to C_{66}. With regard to the longitudinal modes, they found that near T_1 the elastic constant C_{11} shows a steplike anomaly, as does C_{22}, although one of smaller magnitude. Yamanaka *et al.*[15,17] have studied the C_{11} mode with somewhat greater precision. In neither study, however, has an effect on the linewidth been observed. By contrast, our experiments reveal anomalies both in the frequency and the linewidth that are of a shape similar to those found in Rb_2ZnBr_4 near T_1. Figure 9 shows the measured frequencies and linewidths of the C_{11} mode near T_1 in Rb_2ZnCl_4, along with the theoretical curves after fitting to the data. The relevant output parameters of the fit are presented in Table IV. The result for T_1 lies on the higher side of the range of the T_1's obtained from dielectric,[36] specific-heat,[37] and x-ray[38] experiments. As concerns τ^*_A, from Raman experiments[39] we estimate the frequency and linewidth of the amplitudon at a temperature 70 K below T_1 to be about 17 and 8 cm^{-1}, respectively, yielding $\tau^*_A \sim 3\times 10^{-14}$ s, which is an order of magnitude smaller than our result. No other experiment is available providing τ^*_S. An estimate of the ratio $K_2(T_1)/K_1$ can be arrived at in the same way as in the case of Rb_2ZnBr_4. For the effective-mass density of the soft mode we again adopt $0.05\rho_m$, or 0.15×10^3 kg/cm^3.

TABLE III. Output values of fits for the C_{11}, C_{22}, and C_{33} modes in Rb_2ZnBr_4 near T_3.

$\tau^*_<$	$(2.2\pm0.4)\times10^{-13}$ s
$\tau^*_>$	$(1.6\pm0.9)\times10^{-11}$ s
T_3	115.2±0.3 K
$K_2(T_3)/K_1$	0.36±0.12
K_1 (C_{11} mode)	49±3 MHz
K_1 (C_{22} mode)	112±9 MHz
K_1 (C_{33} mode)	61±5 MHz

TABLE IV. Output values of the fit for the C_{11} mode in Rb_2ZnCl_4 near T_1.

τ^*_A	$(2.3\pm0.2)\times10^{-13}$ s
τ^*_S	$(2.1\pm0.9)\times10^{-12}$ s
T_1	303.9±0.5 K
$K_2(T_1)/K_1$	0.65±0.12
K_1	122±5 MHz

The order parameter ρ_0 is taken from the results derived from EPR,[27] Γ is deduced from Raman data,[39] D/μ is set equal to $\sim2\times10^6$ m^2/s^2, and $\omega=2\pi\times11$ GHz. Inserting these values, we arrive at $K_2(T_1)/K_1\sim0.05$, an order smaller than the experimental finding. To estimate K_1, we first calculate, as above, the coupling constant g_1 from the thermal-expansion coefficients,[34] the elastic constants, and $d\rho_0^2/dT$ from EPR,[27] to arrive at $g_1\approx-9.4\times10^{26}$ kg/s^2. Together with $k_i=2.7\times10^7$ m^{-1} and $\rho_m=2.93\times10^3$ kg/m^3, this yields a theoretical K_1 amounting to 80 MHz.

VI. CONCLUDING REMARKS

Brillouin spectroscopy has yielded information on the amplitudon and the soft mode, in particular their relaxation, via the coupling with the acoustic modes. In the analysis of the anomalies at the transition, a quantitative account has been given of both the bilinear and fluctuation parts of the Brillouin shift and broadening. A salient result is that, under the conditions met in a Brillouin experiment, these parts are both of relevance in the compounds considered. This was borne out by the simultaneous fits to the linewidth and frequency data, and, within the uncertainties, substantiated by the theory upon inserting realistic estimates for the parameters. The theory was also able to reproduce the absolute magnitude of the effects.

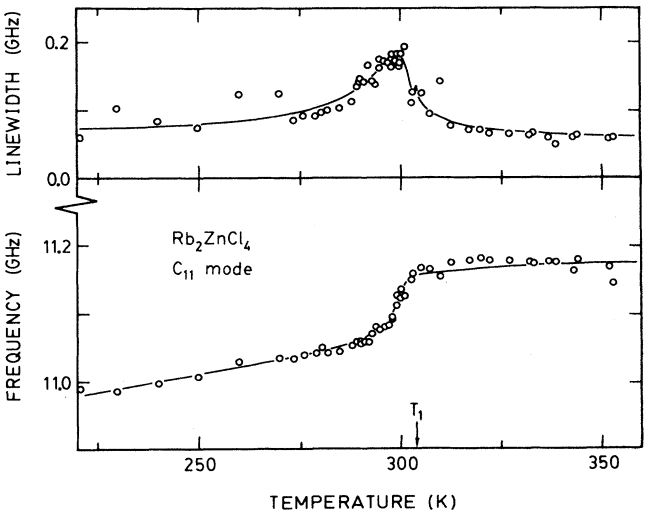

FIG. 9. Frequency and linewidth of the C_{11}-mode acoustic phonon in Rb_2ZnCl_4 near T_1, as measured in the $xy(z,z)\bar{x}y$ scattering geometry. Solid lines are fits.

The linewidth in the incommensurate phase is affected by the amplitudon relaxation primarily through the bilinear term, except very close to the transition. Above the transition, the anomalous linewidth is, of course, solely determined by the fluctuation term. The data allowed to deduce the relaxation of the amplitudon and, to a lesser degree of accuracy, the relaxation of the soft mode. A Landau dependence of the relaxation on temperature was found to be in conformity with experiment. It appeared, however, that the experimental ratios of τ^*_A/τ^*_S, which are of order 0.01 to 0.1, differ from the Landau result 0.5. This is not expected to detract from the conclusions related to the bilinear and fluctuation terms, but rather indicates that in Sec. IV it is likely that too simple an expression for the Landau energy has been used. As concerns the Brillouin frequency, the jump associated with the transition is effectively reduced by the fluctuation term, which, because of the slow decay of its contribution above T_1, cannot be discriminated from the background.

In the treatment of Sec. IV, coupling of the acoustic modes with the phasons has not been incorporated. To account for an interaction between phasons and the longitudinal strains, the energy density, Eq. (6), should be augmented, given that the incommensurate wave vector points along the c^* axis, with symmetry-allowed terms of the form $r_i e_i \rho^2(\partial\phi/\partial z)$.[12] After repeating the derivation of Sec. IV with inclusion of these terms, their bilinear contributions to Eq. (23) turn out to amount to $-r_i^2\rho_0^2k_3^2\chi_\phi^0(\mathbf{k},\omega)$. This result is similar to the expression given by Luspin *et al.*,[16] except for the notable difference of an explicit dependence on the component of the acoustic wave vector along $\mathbf{c}^*$. It implies that effective bilinear coupling to the phason does not show up in the case of C_{11} and C_{22} modes. As for the C_{33} mode, the data in Rb_2ZnBr_4 do not evidence coupling with the phason to be present, and accordingly indicate that its neglect its legitimate.

It is finally of interest to note that the present treatment is equally applicable to the results of ultrasonic experiments conducted at lower frequency. Here, K_2 has gained over K_1 by a factor $\omega^{-1/2}$ [cf. Eq. (33)]. Apart from a compression of the regime of temperatures where the anomalies occur [cf. Fig. 9 and Eq. (34)], therefore, the quadratic fluctuation part dominates the anomalous linewidth and frequency shift. The bilinear part discussed above is reflected primarily in a nearly constant frequency shift and a slow increase of the linewidth already at some distance below T_i. In other terms, the bi-

linear term, which allowed us to derive information on the relaxation of the fluctuations, is diminished relative to the fluctuation part. It should be noted, however, that the increase of the fluctuation term at lower frequencies may to some extent be offset in the event the amplitudon and soft-mode dispersions exhibit a gap at the transition. In this case, τ^{-1} does not drop to zero, but to a finite value τ_0^{-1}. The gap thus becomes noticeable, in particular in the fluctuation part of the linewidth, when the frequency is sufficiently low for $(\omega\tau_0)^{-1}$ to exceed, say, unity. Some knowledge may therefore be gained from a comparison of the ultrasonic velocity of the C_{11} mode in Rb_2ZnCl_4 in the regime near T_1 (Ref. 13) with extrapolations from the present Brillouin study. It then appears that the effect of the fluctuation term is severely overestimated in case a gap is not accounted for. As calculations show, qualitative agreement may be achieved by assuming a τ_0 of order 10^{-9} s.

ACKNOWLEDGMENTS

The authors thank G. J. Dirksen for the growing of the crystals. They further are indebted to Professor A. G. M. Janner for discussions. The work has been supported by the Netherlands Foundations "Fundamenteel Onderzoek der Materie (FOM)" and "Zuiver Wetenschappelijk Onderzoek (ZWO)."

[1]S. Sawada, Y. Shiroishi, A. Yamamoto, M. Takashige, and M. Matsuo, J. Phys. Soc. Jpn. **43**, 2101 (1977).
[2]S. Sawada, T. Yamaguchi, Y. Shiroishi, A. Yamamoto, and M. Takashige, J. Phys. Soc. Jpn. **50**, 3677 (1981).
[3]T. Yamaguchi, S. Sawada, M. Takashige, and T. Nakamura, Jpn. J. Appl. Phys. **21**, L57 (1982).
[4]K. Gesi and M. Iizumi, J. Phys. Soc. Jpn. **45**, 1777 (1978); M. Iizumi and K. Gesi, J. Phys. Soc. Jpn. **52**, 2526 (1983).
[5]A. C. R. Hogervorst and P. M. de Wolff, Solid State Commun. **43**, 179 (1982); A. C. R. Hogervorst, Ph.D. thesis, Delft University, 1986. Here, as well as in the detailed neutron-diffraction investigations of Ref. 4, the modulation in Rb_2ZnBr_4 is inferred not to be genuinely incommensurate, but rather to vary with temperature according to a sequence of large-period superstructures.
[6]C. J. de Pater and C. van Dijk, Puys. Rev. B **18**, 1281 (1978); C. J. de Pater, J. D. Axe, and R. Currat, *ibid.* **19**, 4684 (1979).
[7]T. Ueda, S. Iida, and H. Terauchi, J. Phys. Soc. Jpn. **51**, 3953 (1982).
[8]K. Hamano, T. Hishinuma, and K. Ema, J. Phys. Soc. Jpn. **50**, 2666 (1981).
[9]K. Nomoto, T. Atake, B. K. Chaudhuri, and H. Chihara, J. Phys. Soc. Jpn. **52**, 3475 (1983).
[10]I. A. Belobrova, I. P. Aleksandrova, and A. K. Moskalev, Phys. Status Solidi A **66**, K17 (1981).
[11]R. P. A. R. van Kleef, Th. Rasing, J. H. M. Stoelinga, and P. Wyder, Solid State Commun. **39**, 433 (1981).
[12]V. A. Golovko and A. P. Levanyuk, Zh. Eksp. Teor. Fiz. **81**, 2296 (1981) [Sov. Phys.—JETP **54**, 1217 (1981)]; V. A. Golovko and A. P. Levanyuk, in *Light Scattering Near Phase Transitions,* edited by H. Z. Cummins and A. P. Levanyuk (North-Holland, Amsterdam, 1983), Chap. 3.
[13]S. Hirotsu, K. Toyota, and K. Hamano, J. Phys. Soc. Jpn. **46**, 1389 (1979).
[14]T. Matsuda and I. Hatta, J. Phys. Soc. Jpn. **48**, 157 (1980).
[15]Y. Yamanaka, M. Kasahara, and I. Tatsuzaki, J. Phys. Soc. Jpn. **50**, 735 (1981).
[16]Y. Luspin, M. Chabin, G. Hauret, and F. Gilletta, J. Phys. C **15**, 1581 (1982).
[17]A. Yamanaka, M. Kasahara, and I. Tatsuzaki, Ferroelectrics Lett. **44**, 93 (1982).
[18]A. P. Levanyuk, Zh. Eksp. Teor. Fiz. **49**, 1304 (1965) [Sov. Phys.—JETP **22**, 901 (1966)].
[19]W. Yao, H. Z. Cummins, and R. H. Bruce, Phys. Rev. B **24**, 424 (1981).
[20]W. Rehwald, A. Vonlanthen, J. K. Krüger, R. Wallerius, and H.-G. Unruh, J. Phys. C **13**, 3823 (1980).
[21]M. Cho and T. Yagi, J. Phys. Soc. Jpn. **50**, 543 (1981).
[22]G. Hauret and J. P. Benoit, Ferroelectrics **40**, 1 (1982).
[23]Y. Luspin, G. Hauret, A. M. Robinet, and J. P. Benoit, J. Phys. C **17**, 2203 (1984).
[24]*Landolt-Börnstein, Zahlenwerte und Funktionen,* edited by K.-H. Hellwege and A. M. Hellwege (Springer, Berlin, 1962), 6th ed., Vol. II/8, pp. 2-51, 2-418; *Landolt-Börnstein, Numerical Data and Functional Relationships in Science and Technology, New Series,* edited by K.-H. Hellwege and A. M. Hellwege (Springer, Berlin, 1979), Vol. III/1, pp. 8 and 28; Vol. III/2, pp. 2 and 57; Vol. III/11, p. 29.
[25]C. J. de Pater and R. A. Aptroot, unpublished work quoted in Ref. 6.
[26]A. D. Bruce and R. A. Cowley, J. Phys. C **11** 3609 (1978).
[27]J. J. L. Horikx, A. F. M. Arts, and H. W. de Wijn, Phys. Rev. B **37**, 7209 (1988).
[28]M. Takashige, T. Nakamura, M. Udagawa, S. Kojima, S. Hirotsu, and S. Sawada, J. Phys. Soc. Jpn. **48**, 150 (1980).
[29]E. Francke, M. Le Postollec, J. P. Mathieu, and H. Poulet, Solid State Commun. **35**, 183 (1980).
[30]M. Quilichini, J. P. Mathieu, M. Le Postollec, and N. Toupry, J. Phys. (Paris) **43**, 787 (1982).
[31]N. N. Kolpakova and G. A. Smolenskii, Pis'ma Zh. Eksp. Teor. Fiz. **39**, 545 (1984) [JETP Lett. **39**, 667 (1984)].
[32]M. Wada, H. Shichi, A. Sawada, and Y. Ishibashi, J. Phys. Soc. Jpn. **51**, 3245 (1982).
[33]M. Iizumi, J. D. Axe, G. Shirane, and K. Shimaoka, Phys. Rev. B **15**, 4392 (1977).
[34]I. N. Flërov and I. M. Iskornev, Phys. Status Solidi A **60**, K79 (1980); I. M. Iskornev and I. N. Flërov, Fiz. Tverd. Tela (Leningrad) **25**, 2950 (1983) [Sov. Phys.—Solid State **25**, 1701 (1983)].
[35]S. Sawada. T. Yamaguchi, and N. Shibayama, J. Phys. Soc. Jpn. **48**, 1397 (1980).
[36]K. Hamano, Y. Ikeda, T. Fujimoto, K. Ema, and S. Hirotsu, J. Phys. Soc. Jpn. **49**, 2278 (1980).
[37]B. K. Chaudhuri, K. Nomoto, T. Atake, and H. Chihara, Phys. Lett. **79A**, 361 (1980).
[38]S. R. Andrews and H. Mashiyama, J. Phys. C **16**, 4985 (1983).
[39]M. Wada, A. Sawada, and Y. Ishibashi, J. Phys. Soc. Jpn. **47**, 1185 (1979).